First-principles study of the relations between the elastic constants, phonon dispersion curves, and melting temperatures of bcc Ta at pressures up to 1000 GPa

Michel Foata-Prestavoine
Département de Recherches sur les Matériaux Nucléaires, CEA-Valduc, 21120 Is-sur-Tille, France

Grégory Robert
CEA-DIF, Boîte Postale 12, 91680 Bruyères-le-Châtel, France

Marie-Hélène Nadal
Département de Recherches sur les Matériaux Nucléaires, CEA-Valduc, 21120 Is-sur-Tille, France

Stéphane Bernard
CEA-DIF, Boîte Postale 12, 91680 Bruyères-le-Châtel, France

(Received 6 February 2007; revised manuscript received 18 July 2007; published 14 September 2007)

The possibility to relate analytically elastic shear modulus to melting temperature in the framework of Lindemann melting criterion is investigated here in the particular case of the body-centered cubic phase of tantalum, which is identified as a problematic case. Equation of state, elastic constants, and full phonon dispersion curves (PDCs) are first gathered for a wide pressure range using density functional theory and its perturbation within the generalized gradient approximation. A global fair agreement is found with previous experimental studies. Anomalies in PDCs tend to disappear with compression. Various equivalent Debye temperatures $\theta_D(n)$ are then deduced and compared for increasing compression. The initial Debye model for atomic vibration is found to stand well above 120 GPa. Under this pressure a possibly significant difference up to 10% is found between elastic Debye temperature $\theta_D(-3)$ and $\theta_D(-2)$ required in Lindemann melting criterion. As for all the theoretical melting curves proposed in the past, the one found here using $\theta_D(-2,V)$ completely overpasses the melting curve established by static measurements in diamond anvil cells, but agrees well with the shock melting experiment available. This fact is extensively discussed in terms of evolution of PDCs and explaining hypotheses to be tested in the future are proposed.

DOI: 10.1103/PhysRevB.76.104104 PACS number(s): 62.50.+p, 63.20.−e, 62.20.Dc, 71.15.Mb

I. INTRODUCTION

Two independent and simultaneously published studies[1,2] proposed to relate compression dependence of melting temperature T_m and that of shear modulus G in polycrystalline isotropic monoatomic material. They both invoke the original Debye-model for atomic vibrations[3] and Lindemann melting criterion.[4] In Ref. 1 the relation is expressed in the following simple terms:

$$\frac{G_m(V)V}{T_m(V)} = \chi, \quad \forall\, V. \tag{1}$$

In Eq. (1) χ is considered independent of atomic volume V. The subscript m indicates values taken in the monoatomic solid just before melting. Extensive work of Burakovsky and coauthors on G, T_m, and related quantities,[5–9] including a new analytical model for compression evolution of the Grüneisen parameter,[8] provides useful tools to interpret mechanical and thermal properties of polycrystalline solids. Experimental study of shear modulus near and through the melting temperature at ambient pressure can also be found for some elemental solids,[10,11] but, as mentioned by Burakovsky,[5,6,12] constancy of χ probably fails for some elemental solids before the infinite compression limit because its ambient value is about twice that expected theoretically for the Thomas-Fermi state, which is reached in the compression range 10^2–10^4.[13] Among these problematic metals are body-centred cubic (bcc) Mo, W, Cr, and Ta.

In this study, we intend to inspect detailed evolution of $G(V)$ and $T_m(V)$ of tantalum in the quasiharmonic approximation, and to contribute to the identification of a possible failure of relation (1) in the case of this metal. Tantalum ($Z=73$, and Xe $4f^{14}5d^36s^2$ equilibrium configuration) is a group V A transition metal, like vanadium and niobium. It is stable for pressure up to at least a few megabar,[14–16] and has a very high melting temperature, 3269 K at ambient pressure. Notably, energy-volumes curves of ideal hcp, fcc, A15, and bcc structures proposed in Söderlind *et al.* [15] predict that bcc is stable up to 10 Mbar at least at 0 K. Due to this high mechanical and thermal stability, bcc Ta is a high-pressure standard. A rich history of experimental [17,18] and theoretical[15,19–21] studies exists on its mechanical properties. To discuss relation (1) for bcc tantalum, we use 0 K elastic constants (c_{ij}) and phonon dispersion curves (PDCs) computed from first-principles electronic structure calculations, and experimental data of $T_m(P)$ from literature.[22,23] Calculation of equation of state (EOS), c_{ij}, and PDCs are first presented in detail. Then, PDCs are interpreted in terms of equivalent Debye temperatures which allow us to test melting relation $T_m(V)$ as deduced through Lindemann melting criterion.

TABLE I. Numerical parameters used for the calculations. Energy cutoff and smearing are given in Ha.

Properties	EOS	c_{ij}	PDCs
Cutoff energy	60	60	40
Smearing	0.02	0.02	0.01
Irreducible k-points	440	1100–2200	550–1100

II. CALCULATIONS

A. Computational details

All the *ab initio* results presented here are obtained within density-functional theory (DFT)[24,25] with the Perdew-Burke-Ernzerhof version of the generalized gradient approximation (GGA).[26] We have used the plane-waves formalism plus the separable "dual-space" Gaussian pseudopotential of Hartwigsen, Goedecker, and Hutter (PP-HGH).[27] Five true valence states ($5d^36s^2$) and eight semicore states ($5s^25p^6$) were treated as in Bercegeay *et al.*[28] Gaussian smearing was used and spin-orbit coupling was taken into account for the EOS and elastic constants as recommended by Söderlind *et al.*[15] PDCs calculations were presented in Ref. 28 and negligibility of spin-orbit coupling was checked in this reference. We used the ABINIT code package.[29] Energy convergence tests were performed to determine the cutoff energy, the number of k-points, and the smearing for the Brillouin zone (BZ) integration for the whole compression range, depending on the properties addressed. Table I summarizes these numerical data.

B. Equation of state

We calculated the total energy for 17 undeformed unit cells with volumes spanning from 18.5 to 8 Å^3. 0 K equation of state is calculated by local least-squares fits of these $E(V)$ data points from the relation $P=-(\partial E/\partial V)_{T=0\ \mathrm{K}}$. Figure 1 presents the corresponding $P(V)$ data. The equation of state of Ta has been extensively studied by several experimental techniques and *ab initio* DFT electronic-structure calculations.[15,19] Figure 1 compares our calculations with diamond anvil cell (DAC) experimental data of Dewaele[18] and shock-wave experiments.[30] Thermal pressure between 0 K calculations and ambient DAC experiments is about 1.3 GPa over the whole compression range according to Cohen *et al.*[19], so it can be safely neglected. If we follow Dewaele's recommendation to take into account the Holzapfel modification of Ruby scale,[31] diamond anvil cell (DAC) and shock-wave experiments are in perfect concordance. We confirm[28] here the excellent agreement between $P(V)$ data computed with the PP-HGH-GGA method and experiments.

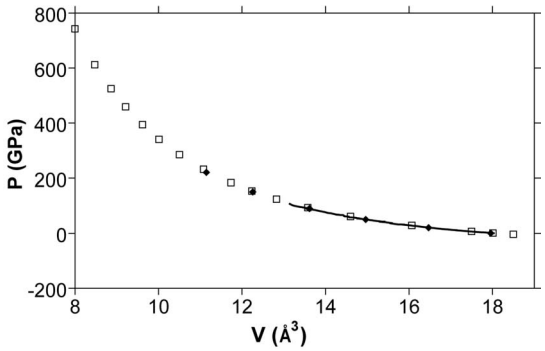

FIG. 1. Pressure-atomic volume relationship according to PP-HGH-GGA calculations (large open squares), reduced shock-wave measurements (Ref. 30) (closed diamonds), and diamond anvil cell experiments of Dewaele (Ref. 18) with modified ruby pressure scale after Holzapfel (thick line).

C. Elastic constants

For each volume of the unit cell, the complete set of the bcc Ta elastic constants (c_{11}, c_{12}, c_{44}) and pressure were deduced from a least-squares fit of the strain energy for particular deformations[32] listed in Table II. For each strain type, eight symmetric values of δ in the range ±5% were used to make the strain energy fit. The results of these calculations are presented in Table III and Fig. 2. Since five deformations are used to fit four unknown parameters (c_{11}, c_{12}, c_{44}, and P), two values for each parameter are derivable. Because of symmetry relations in a bcc crystal, perfectly converged energy calculations should give two identical values. In Table III, only median values are given. For P, mean value takes also into account the value calculated from local fits of $E(V)$ data. Differences between the three P values never exceed 0.1 GPa and are therefore negligible. For c_{11} and c_{12} differences do not exceed 1.5% over the whole compression range. Noticeable differences exist only for c_{44} as shown in Fig. 2. Particularly, it should be noted that the difference increases and reaches approximately 16 GPa between 150 and 250 GPa. Then it decreases very slowly. We remarked also that convergence of c_{44} values with respect to k-points

TABLE II. Strain tensors employed for computation of elastic constants, and associated strain energy formula. ε is a 3×3 symmetric tensor; unspecified ε_{ij} are 0.

Strain tensors	Energy formula
$\varepsilon_{11}=-\varepsilon_{22}=\delta$; $\varepsilon_{33}=\delta^2/(1-\delta^2)$	$\Delta E/V=(c_{11}-c_{12})\delta^2+o\{\delta^3\}$
$\varepsilon_{12}=\delta/2$; $\varepsilon_{33}=\delta^2/(4-\delta^2)$	$\Delta E/V=(c_{44}/2)\delta^2+o\{\delta^3\}$
$\varepsilon_{11}=\varepsilon_{22}=\delta$	$\Delta E/V=-2P\delta+(c_{11}+c_{12}-P)\delta^2+o\{\delta^4\}$
$\varepsilon_{33}=\delta$	$\Delta E/V=-P\delta+(c_{11}/2)\delta^2+o\{\delta^4\}$
$\varepsilon_{13}=\delta$	$\Delta E/V=(2c_{44}+P)\delta^2+o\{\delta^4\}$

TABLE III. Zero temperature EOS and c_{ij} calculated at the 17 volumes considered. Volumes are in Å^3, energy of unstrained bcc cells is in Ha, and pressures and c_{ij} are in GPa.

V	$E_{\text{unstrained}}$	P_m	c_{11m}	c_{12m}	c_{44m}
18.5000	−59.1691811	−4.0	238.5	149.8	64.6
18.0109	−59.1690056	1.0	263.6	165.8	69.8
17.5000	−59.1687265	6.9	292.3	184.1	75.4
16.0680	−59.1631329	28.5	390.1	247.2	93.3
14.6015	−59.148415	61.2	525.8	336.7	115.7
13.5784	−59.1304681	93.3	652.8	421.3	136.3
12.8282	−59.1118717	123.9	772.0	500.0	156.6
12.2372	−59.0931263	153.5	888.9	575.7	178.6
11.7362	−59.0738033	183.5	1009.7	652.4	203.5
11.0788	−59.0426357	231. 7	1208.3	777.0	248.8
10.5025	−59.0086289	284.8	1427.7	916.6	303.7
10.0123	−58.9735759	340.5	1652.3	1064.5	363.3
9.6170	−58.940344	394.1	1862.3	1207.7	421.1
9.2142	−58.9010331	458.8	2108.3	1380.6	490.3
8.8645	−58.8616483	524.8	2354.3	1558.1	560.4
8.4739	−58.8108389	612.1	2671.8	1795.3	651.1
8.0000	−58.7374978	742.2	3132.2	2156.4	783.1

sampling of the BZ is also more difficult in this compression range.

Studies of compression dependence of elastic constants exist in literature. Experimentally, there have been near ambient-pressure ultrasonic measurements[17] and measurements up to 105 GPa by stress/angle-resolved x-ray diffraction (SAX) in diamond anvil cells (DAC).[14] Elastic constants were also computed, first at 0 K in the 0–10 Mbar range, from a full-potential method with linear muffin-tin orbital (FP-LMTO),[15] and second in the [0–10^4 K, 0–450 GPa] range by a full potential linearized augmented plane wave method (FP-LAPW) associated with a particle-in-a-cell procedure.[20] All c_{44} and tetragonal shear constant $c_s=(c_{11}-c_{12})/2$ issued from these references are presented in Fig. 2.

Due to uncertainties in DAC-SAX experiments, it is difficult to discuss the agreement with them. Our elastic c_{ij} are mostly within error bars of the experimental values, except for c_{44} at low pressures which is underestimated here, like in Gülseren *et al.* (by 16%). This error is probably underestimated by a few percents as we are comparing 0 K calculations to experimental data at ambient temperature.

Agreement with the first principle results of Söderlind *et al.* or Gülseren *et al.* is reasonable as a whole; but some differences must be noticed. First, above 400 GPa, values for c_{44} diverge appreciably; but pressures considered in Gülseren *et al.* do not exceed 450 GPa. The difference of 10% for c_{44} with Söderlind *et al.*; at the highest pressure considered here, is not highly significant given classical divergences of *ab initio* methods at high pressures. More interesting to mention is the evolution of elastic shear moduli between 100 and 250 GPa. In this range, the FP-LAPW study of Gülseren *et al.* reported a strong softening of c_{44} but no softening of c_s, so that anisotropy ratio c_{44}/c_s even passes transitorily under unity in this interval. On the other hand, the PP-HGH-GGA method used here, theoretically more precise, predicts hardly any softening of c_s and very smoother softening of c_{44}. The DFT method used in the study of Söderlind *et al.*,[15] related in different papers later,[33,21] is theoretically the finest of the three methods. According to the values of c_{44} and c_s at 193 GPa presented in some of these references (Fig. 2), softening is noticeable for both shear elastic constants. But it is worth noting in this study that 193 GPa is the only pressure considered in the range 100–250 GPa. Moreover, in Ref. 21, the model generalized pseudopotential theory (MGPT) multi-ion potential constructed by the authors just misses these values for c_{44} and c_s.

This high variability of shear elastic constants, and of c_{44} in particular, when calculated by different *ab initio* methods in this pressure range is somehow confusing. Indeed, EOS of all the studies mentioned are in good agreement with ours, and show no peculiar evolution in this compression range. Gülseren and Cohen[20] attributed the softening of c_{44} to a major reconfiguration of the Fermi surface evidenced between 5 and 460 GPa[19] and concluded that elastic constants can be much more sensitive to changes in the Fermi surface than the equation of state. This major transformation of the electronic structure in the first few hundred GPa was also observed during this study. Similarly, we note that softening of c_{44} was very sensitive to convergence with respect to k-points sampling and smearing in PP-HGH-GGA calculations, unlike other elastic moduli and EOS. Then, trigonal shear strain energy, corresponding to c_{44}, may be particularly dependant on peculiar structures in the electron energy at the Fermi surface, and these structures may be fine enough to require detailed sampling of the Brillouin zone to be correctly reproduced. Consequently, c_{44} would naturally be also very sensitive to the DFT method employed. We will observe similar effects in phonon dispersion curves hereafter.

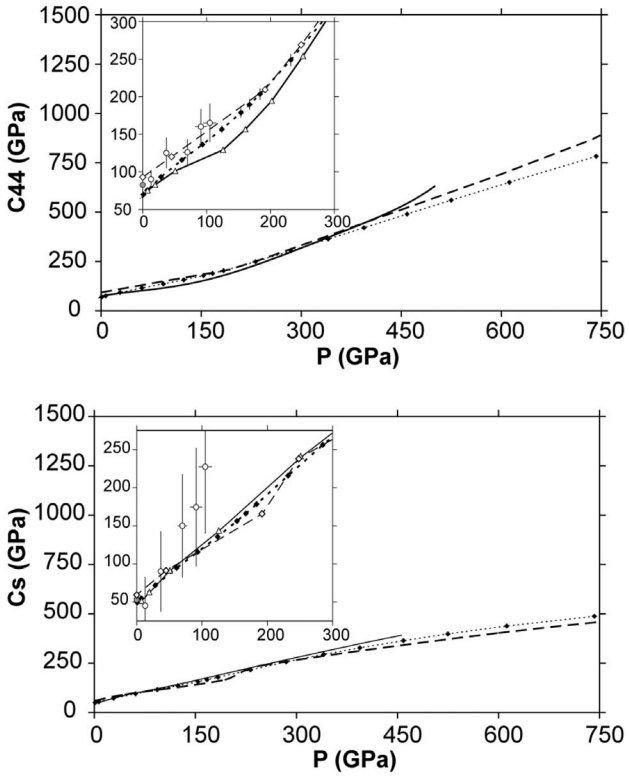

FIG. 2. (a) Elastic c_{44} and (b) elastic c_s for Ta: closed diamonds and dotted line are for mean values of these 0 K PP-HGH-GGA calculations (c_{44} error bars in the inset indicate the two values when distinguishable). Open circles are for experimental SAX values of Cynn *et al.* (Ref. 14). Closed circle is for ambient ultrasonic measurement (Ref. 17). Open diamonds and long dashed lines are for 0 K FP-LMTO calculations of Söderlind *et al.* (Ref. 15). Open triangles and thick lines are for FP-LAPW computations of Gülseren *et al.* (Ref. 20). In the inset, the values of c_s and c_{44} shown at 193 GPa of Söderlind *et al.* were ignored in Ref. 15, but featured in a subsequent paper (Ref. 21) by the same authors.

D. Phonon dispersion curves

The calculated phonon dispersion relations discussed here in detail have already been presented by Bercegeay *et al.*[28] They were obtained in the framework of density functional perturbation theory (DFPT).[34,35] The strategy is to construct the full dynamical matrix corresponding to a wave vector q in the BZ, containing the second derivatives of the energy with the displacement of the atom. The three eigenfrequencies of this matrix are the three phonon vibrations modes for this q vector. In DFPT, the strain of the crystalline unit cell corresponding to each phonon state is described in the Born-Oppenheimer approximation, as a static perturbation to the electronic structure which is self-consistently calculated. Doing this on a fine enough mesh of q vectors in the BZ, the dispersion curves along the symmetry direction and the phonon density of states (PDOS) can be interpolated by a Fourier procedure. Computational parameters reported in Table I were used, and a mesh of $8\times8\times8$ q points in the BZ corresponding to 29 vectors in the irreducible BZ was considered for interpolation. This was done for the following five compression values: 1.00, 1.25, 1.39, 1.96, and 2.51, corresponding approximately to 0, 60, 120, 450, and 1000 GPa, respectively, according to our equation of state.

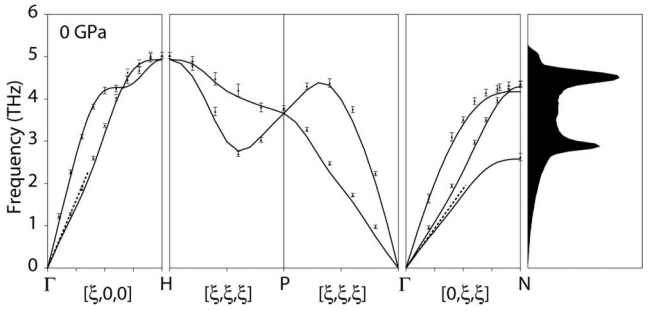

FIG. 3. $P=0$ phonon dispersion curves of Ta. Symbols with error bars are from Woods (Ref. 36), and lines are DFPT calculations. The corresponding phonon density of states is shown at the right.

PDCs of bcc transition metals of group V A (V, Nb, and Ta) and VI A (Cr, Mo, and W) show numerous anomalies with respect to PDCs of standard bcc metals. Born-von Karman fits to these generally extend at least to seven nearest neighbors, indicating complicated long distance and angular dependences of atomic force constants. The comparison of the PDCs calculated at $P=0$ with dispersion relations measured in ambient conditions by Woods[36] is fair as presented in Fig. 3. The peculiar points to notice on PDCs are the following.

(1)The crossing over of acoustic longitudinal (L) and transverse (T) branches due to a softening of the longitudinal mode around $\xi\approx0.7$ along the $[\xi,0,0]$ direction.

(2)The pronounced changes in slope for $\xi\approx0.5$ and 0.75 along the $[\xi,\xi,\xi]$ T branch.

(3)The increase in the $d\omega/d\xi$ value which occurs at about halfway across the zone for the $[\xi,0,0]$ T and $[0,\xi,\xi]$ T2 branches.

(4)The decrease below the elastic constants line (dashed line near Γ points in Fig. 3) near $\xi=0.25$ for the $[\xi,0,0]$ T branch.

(5)The high lying $[0,\xi,\xi]$ T2 branch which does not cross over the $[0,\xi,\xi]$ T1 branch. This is coherent with the observation that c_{44} is greater than c_s in Ta (Fig. 2), and that the calculated T2 phonon frequency is much greater than T1 phonon frequency at the N point of the BZ boundary (Fig. 4).

Features (1)–(4) are common with Nb PDCs.[37] Anomalies (1) and (2) are clearly seen on both experimental and calculated PDCs of Ta. The third anomaly is also noticeable but much less important than the two previous. The fourth is also a well-known anomaly of Nb PDCs. It is visible on the computed PDCs of Ta but in the study of Woods the sampling of the BZ is not fine enough to confirm or infirm it experimentally. The last anomaly is very distinctive of Ta with respect to PDCs of other group V A and V I A bcc transition metals.

The minus three, zero, first and second equivalent Debye temperature $\theta_D(n,V_0)$ corresponding to the $P=0$ PDCs for tantalum are also in good agreement with their available measured values by various experimental tools,[38,39] as shown in Table IV. We verify also here that $\theta_D(-3,V_0)$, calculated from computed PDCs, is sensibly greater than all other

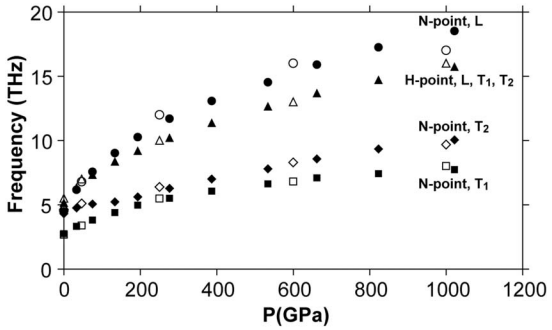

FIG. 4. Phonon frequencies calculated at the H and N points for 11 different compressions and comparison to frozen-phonon calculations in Söderlind *et al.*(Ref. 15). Triangles are for degenerated modes in H point, dots are for the longitudinal mode in N point, squares and diamonds are, respectively, for the first and second transversal modes in N points. Closed symbols represent calculations of this study and open symbols are results from Ref. 15.

known $\theta_D(n,V_0)$. This constitutes a significant departure from the Debye first model for atomic vibrations, according to which all PDCs follow a unique linear dispersion law, which implies equality of all $\theta_D(n,V_0)$. This is also coherent with anomaly (4) mentioned above which makes the initial slope of PDCs in the central BZ sensibly greater than the mean slope over the rest of the PDCs.

With compression, phonon frequencies calculated can be compared to the frozen-phonon calculations done by Söderlind *et al.*[15] at H and N high-symmetry points of the BZ. Again, the agreement presented in Fig. 4 is good except for longitudinal N point frequency above 400 GPa.

Thanks to the good agreement of calculated PDCs with both ambient experiments and available calculations in pressure, we can now inspect rather confidently their detailed evolution with compression. With decreasing volumes, anomalies reported above tend to disappear, giving dispersion curves typical of normal bcc elements (Fig. 5). One important modification in the PDCs is the relative lowering of the $[0,\xi,\xi]$ T2 branch with respect to the longitudinal mode along the same direction. Then, with compression, anomaly (5) reported above disappears and tantalum gets back the classical two low lying shear modes of bcc lattices in the $[0,\xi,\xi]$ direction, and the corresponding shape of the low frequency part of the PDOS. In the mean time one observes relative elevation of other branches of the spectrum, namely the $[\xi,\xi,\xi]$ T branch (vanishing of second anomaly), the central part of the $[\xi,0,0]$ L branch (vanishing of first anomaly), and also quite a noticeable elevation of the $[0,\xi,\xi]$ L branch near the BZ border, which becomes the highest part of the spectrum. Finally, one can also notice that slight anomalies (3) and (4) also disappear from PDCs.

TABLE IV. Comparison of the available experimental value of Debye temperatures with those derived from the first-principles calculated $P=0$ PDCs. Unity is Kelvin (K).

At $P=0$	$\theta_D(-3)$	$\theta_D(0)$	$\theta_D(1)$	$\theta_D(2)$
Present calculation	247.0±5.0	218.7	218.6	218.9
Experiment (Ref. 38)	258	229		
Experiment (Ref. 39)			217.0±2.0	217.0±2.0

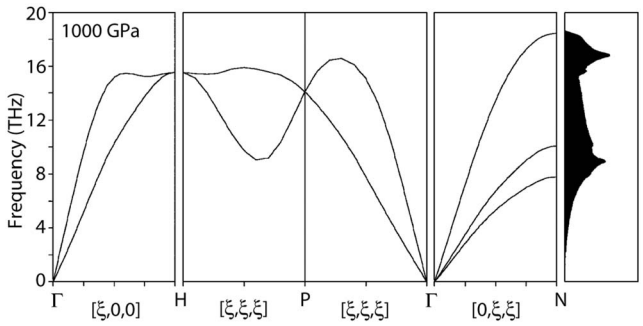

FIG. 5. $P=1000$ GPa phonon dispersion curves of Ta calculated within DFPT. At this high pressure, PDCs of Ta present the typical regular shape for normal bcc elements.

Figure 6 represents the PDOS deduced from PDCs for the five compressions considered. Frequencies are reduced to the highest frequencies ω_{max} of each PDOS to get easier comparison, independently of the natural extension of the spectrum to the high frequencies due to the increase of strain-energy with pressure. One can clearly see important modifications in the detailed shape of PDOS at various frequencies, corresponding to the evolution of anomalies mentioned before. Disappearance of anomaly (5) corresponds to the progressive broadening of the first high in the PDOS ($\omega/\omega_{max}\approx 0.5$). As quoted before by Zener,[40] this strengthens the weight of the PDOS at low ω. On the other hand, as shown on the PDCs, vanishing of anomalies (1) and (2) and relative elevation of the $[0,\xi,\xi]$ L branch strengthen the high-frequency content of the spectrum.

The PDOS at different compressions presented above are the basic tool for the analysis hereafter. Indeed, if anharmonicity is not too important at the temperature considered,

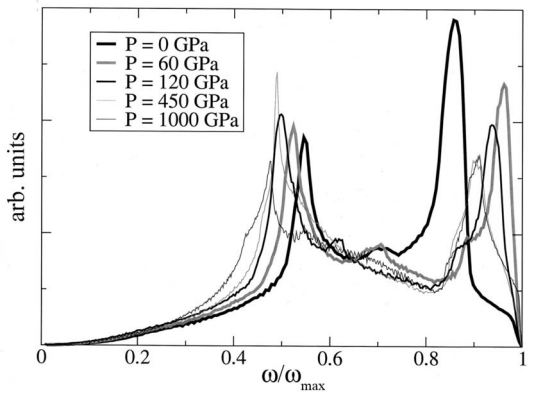

FIG. 6. Phonon density of state calculated at five pressures. Frequencies are reduced to the highest frequencies ω_{max} of each PDOS. $\omega_{max}=5.006$ THz for $P=0$ GPa, 7.045 THz for $P=60$ GPa, 8.484 THz for $P=120$ GPa, 13.730 THz for $P=450$ GPa, and 18.557 THz for $P=1000$ GPa. Note the relative strengthening of the highest and lowest frequency contents, at increasing pressure.

more than rough approximations of numerous thermal and mechanical properties can be deduced from quasiharmonic treatment of the PDOS calculated at 0 K.[38] Then we will now see what can be inferred in terms of melting temperature $T_m(V)$ and $G(V)$.

III. IMPLICATIONS FOR RELATION BETWEEN $T_m(V)$ AND $G(V)$

A. Theoretical understatements of relation (1)

Relation (1) requires essentially two conditions. First, it invokes the Lindemann melting criterion according to which a solid melts when atomic mean square vibration $\langle u^2 \rangle$ reaches a fixed fraction of the mean interatomic distance.[4] For temperatures above Debye temperature ($\sim$230 K in the case of Ta) harmonic mean square atomic vibration $\langle u^2 \rangle$ is related to the −2 equivalent Debye temperature $\theta_D(-2,V,T_m)$. This leads to the most commonly used version of the Lindemann criterion:

$$\frac{T_m(V)}{V^{2/3}\theta_D^2(-2,V)} = \text{cst}, \quad \forall\, V. \tag{2}$$

Second, relation (1) requires volume dependence of $\theta_D(-2,V)$ to be collinear to that of the −3 equivalent Debye temperature $\theta_D(-3,V)$. Rigorously, $\theta_D(-2,V)$ is proportional to the second frequency moment of atomic vibrations. It is then deduced from integration of PDCs spanning all over the first Brillouin Zone (BZ). On the other hand, $\theta_D(-3,V)$ averages only the initial dispersion coefficients at the Γ point of BZ, that is to say monocrystalline elastic constants (c_{11}, c_{12}, and c_{44} in case of a cubic crystal). A very simple relation exists between $G(V)$ and $\theta_D(-3,V)$,[9,38]

$$\theta_D(-3,V) \approx \left(\frac{9\pi^2}{V}\right)^{1/3} \frac{\hbar}{k_B} \sqrt{\frac{G(V)}{\rho}} \pm 5\ \%\ , \tag{3}$$

where V is atomic volume, $\hbar$ reduced Planck constant, k_B Boltzmann constant, and ρ density. This relation is much more precise than its bulk modulus counterpart invoked in Slater's form of the Grüneisen parameter.[41] The reason is that it is analytically much less dependent on the variation of Poisson ratio with compression. Note also that this relation requires no other theoretical approximation except negligibility of anharmonicity if nonzero temperatures are considered. Then supposing $\theta_D(-2,V)/\theta_D(-3,V)=$cst, relations (2) and (3) give relation (1).

Just above, relation (1) has been introduced in the quasiharmonic framework for simplicity. Then, shear modulus and nth equivalent Debye temperatures were treated as temperature independent quantities on isochors. This is a rather wrong hypothesis in general.[38] To be valid relation (1) should be considered with $G(V)$ and moments frequencies evaluated near melting. However, in a first approximation, it is possible to test the hypothesis above thanks to the c_{ij} and PDCs calculated at 0 K, with relatively simple corrections of quasiharmonic relations. In the Preston-Wallace model,[42] temperature dependence of shear modulus between 0 K and melting temperature is written

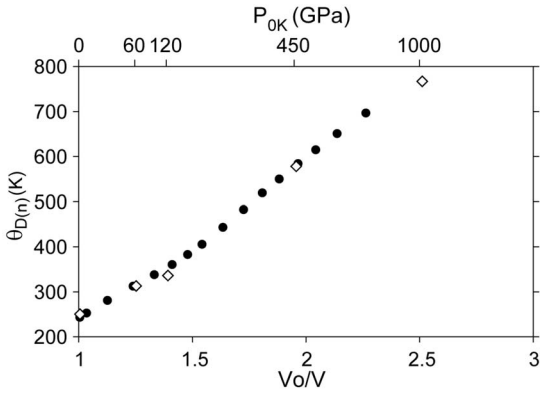

FIG. 7. Minus three equivalent Debye temperature deduced from elastic constants calculations $\theta_{DVs}(-3)$ (dots) and from PDCs $\theta_{DPh}(-3)$ (diamonds). Both methods give a similar value. Cold pressures corresponding to the PDCs calculations are reported on the top axis.

$$\frac{G(V,T)}{G(V,0)} = 1 - \beta\frac{T}{T_m}. \tag{4}$$

The linearity was verified experimentally over the accessible range between θ_D and T_m for a wide variety of monoatomic crystals, and statistically, β was found[42] equal to 0.23 ± 0.08. Burakovsky *et al.*[1] found similar values when modeling behavior of the infinite pressure limiting Thomas-Fermi state. Then, as initial and expected final values of β hardly differ over 2–4 decades of compression, it is proposed in Ref. 1 to regard β as density independent. Consequently $G_m(V) \propto G(V,T=0)$, and relation (3) implies $\theta_D(-3,V,T=0) \propto \theta_D(-3,V,T_m)$. Similarly, one can suppose that $\theta_D(-2,V,T=0)$ scales with $\theta_D(-2,V,T_m)$ whatever compression is considered. Then, relation (1) can stand in a more realistic anharmonic model if we only suppose that temperature induced relative losses of $\theta_D(-2)$ and $\theta_D(-3)$ between $T=0$ and melting are independent of the isochors considered.

We will now derive the evolution with compression of various nth Debye temperatures $\theta_D(n,V)$ from the calculated PDOS and see, in particular, if $\theta_D(-2,V)/\theta_D(-3,V)$ is constant as understated in relation (1).

B. Evolution of various $\theta_D(n,V)$ with compression

$\theta_D(n)$ are defined for $n \in [-3,+\infty]$. Complete definitions can be found in Ref. 38. For $n \geqslant -2$, $\theta_D(n)$ is deduced from the calculation of the moment frequency $\langle \omega^n \rangle^{1/n}$ using the whole PDOS presented in Fig. 6. On the other hand, $\theta_D(-3)$ can be deduced either from elastic constants calculations using Debye average for sound velocity, or from the least-squares fit of the divergent behavior of the PDOS with the suitable following form:[38] $F(\omega)=a_1\omega^2+a_2\omega^4$. Hereafter these two values will be noted $\theta_{DVs}(-3)$ and $\theta_{DPh}(-3)$, respectively. The best fit for $\theta_{DPh}(-3)$ was obtained when considering the region $\omega \leqslant 0.2\omega_{\max}$ of the PDOS. Uncertainty of the fit was always inferior to 10 K. $\theta_{DVs}(-3)$ and $\theta_{DPh}(-3)$ are represented in Fig. 7 for the whole compression range considered, and the expectable global agreement is verified.

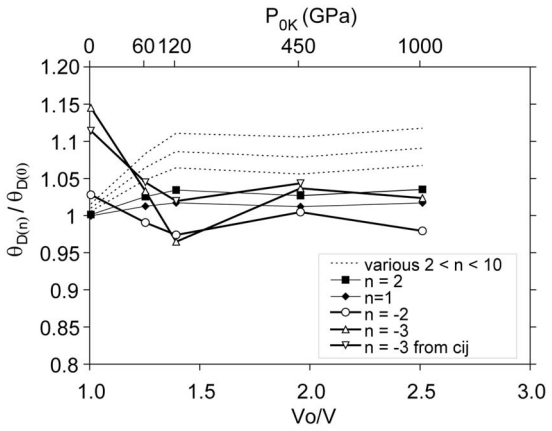

FIG. 8. Relative variation with compression of various $\theta_D(n,V)$ calculated with PDOS reduced to $\theta_D(0,V)$. $\theta_{DVs}(-3)$, deduced from c_{ij}, is included for comparison with $\theta_D(-3)$. Pressures at 0 K are reported on the top axis.

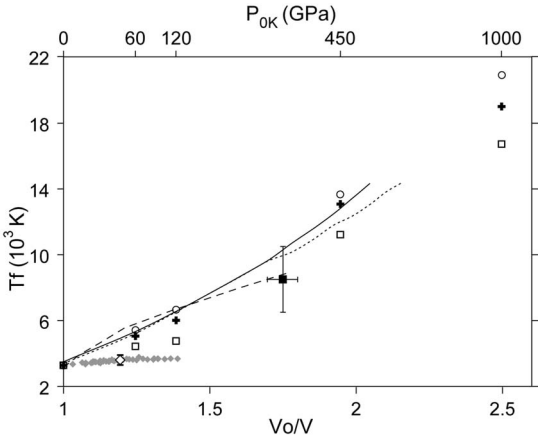

FIG. 9. Melting temperatures of Ta according to experiments in DAC with the laser heating device of Errandonea (Ref. 22) (gray little diamonds), our experiment at 35 GPa (large open diamond), an estimate from shock measurement of Brown around 300 GPa (Ref. 30) (closed square), various published theoretical studies from Refs. 43–45 (dotted, continuous, and dashed lines, respectively), and values deduced from the Lindemann melting criterion and PDOS of this study using either $\theta_D(-2,V)$ (crosses), or $\theta_{DPh}(-3,V)$ (open squares), or $\theta_D(0,V)$ (open circle). Pressures at 0 K corresponding to the isochors considered in PDCs calculations are reported in the top of the figure.

The evolutions with compression of various nth $\theta_D(n,V)$ are now compared. First, only $\theta_D(n,V)$ related to the PDOS are considered. Values of $\theta_D(n,V)$ reduced to $\theta_D(0,V)$ are illustrated in Fig. 8. Within the [1–1.38] compression range (0–120 GPa), $\theta_D(n,V)$ increases faster than $\theta_D(n',V)$ if $n > n'$. This can be simply correlated to the modification of PDCs described before. Indeed, as quoted before, vanishing of the anomalies in the low frequency part of the spectrum tends to strengthen the low frequency contents of the spectrum whereas evolution of the high frequency part of the spectrum has the opposite effect. Due to the definitions of the $\theta_D(n,V)$, the bigger n is, the less $\theta_D(n,V)$ will be influenced by the evolution of the low frequency part of the PDCs. Then it is natural that the bigger n, the faster is the increase of the corresponding moment frequency $\langle\omega^n\rangle^{1/n}$ and Debye equivalent temperature $\theta_D(n,V)$.

Figure 8 shows that PDCs calculated predict that $\theta_D(-3,V)$ decreases, in ratio to $\theta_D(-2,V)$, of approximately 11% within the [1–1.38] compression range. Eleven percent variation is not huge, given fundamental uncertainties in *ab initio* calculations. If we now look at the evolution of $\theta_{DVs}(-3)$ (deduced from c_{ij}), differences with $\theta_D(-2,V)$ are even much smaller. So, if we consider that an estimation of some kind of uncertainty on $\theta_D(-3,V)$ is given by the difference between $\theta_{DVs}(-3)$ and $\theta_{DPh}(-3)$, then it would not be too rough an approximation to regard $\theta_D(-2,V)/\theta_D(-3,V)$ as constant, at least above 1.25 or 1.38 compression. This means that, in this relatively high compression range, no highly significant differences are expected when using $\theta_D(-3,V)$ or $\theta_D(-2,V)$ in Eq. (2) to estimate $T_m(V)$ with the Lindemann melting criterion.

A similar conclusion can be drawn about $\theta_D(n,V)$ for $n \in [-1,4]$. In particular, $\theta_D(0,V)$ and $\theta_D(2,V)$, which determines the free energy in the classical limit, are nearly proportional to each other on the whole compression range. Quasiharmonic estimation of the thermal ionic contribution to many physical properties such as thermal expansion should then be possible using a unique Debye temperature up to 1000 GPa, like in the very simple initial Debye model for atomic vibration.

C. Melting temperature

Interest on bcc tantalum, as well as on the other bcc transition metals of group V A (V, Nb, and Ta) and VI A (Cr, Mo, and W), has been revived recently by the first measurements of their melting temperatures T_m up to 100 GPa,[22] with a laser-heating and diamond anvil cell (DAC) device. A very rapid flattening of melting curves $T_m(P)$ in the first 50 GPa with nearly constant T_m above has been observed. This is in clear disagreement with all the various theoretical models and calculations for Ta,[43–45] Mo,[12] and W,[7] and difficult to conceal with the high pressure shock melting studies.[22,23] These discrepancies are illustrated in Fig. 9 together with melting temperatures from this work. Using relation (2) with $\theta_D(-2,V)$ we have found melting temperatures $T_m(V)$ indicated by thick crosses. In comparison with this melting curve deduced from $\theta_D(-2,V)$ as required by the Lindemann melting criterion (2), the one deduced from $\theta_D(-3,V)$ on the whole compression range leads to a significant underestimation of Tm between 1 and 1.25 compression (open squares in Fig. 9). This is the straightforward consequence of the relative softening with compression of shear modes in central BZ and vanishing of the fifth anomaly. $\theta_D(-3,V)$ averages these modifications of elastic phonons in the central part of the BZ and does not integrate the other modifications of PDCs which affect simultaneously the other branches of the spectrum. As Wallace argues for $\theta_D(0)$ as the relevant moment in the Lindemann rule,[46] melting temperatures deduced

from relation (2) with $\theta_D(0,V)$ are also represented in Fig. 9 for comparison.

Like previous theoretical models for melting temperatures of Ta, values obtained here using the Lindemann melting criterion together with precise 0 K calculations of $\theta_D(-2,V)$ or $\theta_D(0,V)$ are coherent with shock-melting temperature measurement around 300 GPa, but they do not better match low pressure experimental data from Errandonea.[22] A measurement of T_m at 35 GPa was made during this study in our laboratory, using a DAC and laser heating device similar to that of Errandonea.[22] Here is briefly described our experimental procedure. Pressure transmitting medium in the DAC is argon. The pressure is estimated at ambient temperature by ruby luminescence. The tantalum sample is approximately 80 μm wide and 40 μm thick. To heat the sample, a continuous YAG laser is focused at its surface. The spot is approximately 25 μm wide. Temperature measurement is achieved on the same surface by the spectrometry method all along a line crossing the spot at it center. This permits us to measure the horizontal temperature gradient. Temperature is approximately homogenous and maximal only on a 10 μm wide area in the center, and then it diminishes dramatically toward the exterior of the spot. During the experiment, laser power is progressively increased and temperature is measured continuously in the meantime. When power of the laser is sufficient, the solid melts at the center of the spot, which cause a change in the power-temperature relation observed. Liquid phase is also commonly pushed out of the place, which leaves a characteristic hole in the sample. Three combined melting criteria are used. The speckle method and laser power-temperature relation permit recognition of melting during the experiment.[47–49] After opening the diamond anvil cell, a hole in the sample at the position of the spot confirms its melting. Using the apparatus described just above, we confirmed a very low melting point for bcc Ta at moderate pressure as compared to theoretical estimations (Fig. 9).

We have no precise theoretical explanation for systematic deviation of experimental melting temperatures below 100 GPa and theoretical values of this study. We have noted important modifications in the PDCs in the pressure range where experiments of Errandonea[22] report melting temperatures much smaller than theoretical estimations; but even if modifications of the low frequency part of PDCs in the first 120 GPa [vanishing of anomaly (5) and possible softening of c_{44}] should lower $\theta_D(-2,V)$, the effect is compensated by simultaneous disappearance of anomalies (1) and (2) and elevation of the $[0,\xi,\xi]$ L branch. Then hardly any lowering is visible on the melting curve deduced from the Lindemann melting criterion with $\theta_D(-2,V)$. On the contrary when using $\theta_D(-3,V)$ between 0 and 120 GPa in Eq. (2), Tm tends to be significantly lowered. This is straightforwardly the consequence of that $\theta_D(-3,V)$ averages the modifications of elastic phonons only, in the central part of the BZ, and does not integrate the other modifications of PDCs.

One can question the validity of the Lindemann melting criterion. This is a one phase melting criterion. Like all one phase criteria, its validity is rightly debated. Rigorously, only equality of the free energy of the two phases should be considered. In practice, however, as shown by Ross on Mo,[50] free energy curves of solid and liquid phases can almost coincide with each other. As modeling of these free energies contains a number of adjustable parameters, a slight variation of one of them may shift the critical temperature away from its correct value. In the study of Ross, it is evidenced that a small broadening of the d-band width ($\sim 1\%$), in a particular model for the liquid phase, leads to an increase in the stability of the liquid relative to the solid sufficient to depress the melting to a value in agreement with the recent diamond-anvil cell measurements of Errandonea.[22] This is supposed by Ross to be a quite typical situation in transition metals. Hence as fine-tuning of the free parameters for solid and liquid tantalum are hardly achievable, the numerous recorded success of the Lindemann melting criterion still make it a worth testing hypothesis.

Another possibility is to address the hypothesis we have made that $\theta_D(-2,V,T=0)$ scales with $\theta_D(-2,V,T=T_m)$ at every compression considered. As explained before, this hypothesis corresponds to a very simple but usual approach[21] for anharmonicity which might deserve questioning. Similarly, if we refer to the melting criterion in terms of $\theta_D(0)$ proposed by Wallace,[46] this would lead one to suspect that $\theta_D(0,V,T=0)$ does not scale with $\theta_D(0,V,T=T_m)$ at all compressions, in other words that the relative anharmonic increase of entropy of the solid with temperature up to melting can be very different at low and at high compression.

The experimental device might also deserve some attention. Belonoshko *et al.*,[12] facing the same difficulty to predict laser-heating DAC experiments on molybdenum, argued that this technique, based on the visual observation of an emerging phase, leads to an erroneous conclusion. Precisely, it was proposed by the authors that, in DAC experiments of Errandonea,[22] a solid-solid transition was misinterpreted as melting; but in the case of Ta, no such stable phase is predicted at low temperature below 1000 GPa.[15] A high-T solid-solid transition at lower pressure cannot be totally excluded, but we firmly believe that the transition identified in DAC experiments is melting. First, Errandonea used angle-dispersive x-ray diffraction to identify bcc and liquid phases.[22] The hole observed in the sample, at the end of our experiment in DAC, confirmed that melting was reached. It was also proposed that important thermal stress in the sample may produce dynamic recrystallization, which may be interpreted as onset of convectivelike motion at lower temperatures than melting temperature.[51] Such a recrystallization process may indeed take place during laser-heating experiments in DAC, but it probably cannot create the hole we observed in the sample at the end of the experiment. Finally, the fact that the temperature measured at the drastic onset of clear speckle motion in DAC evolves continuously toward the exact value of melting temperature in ambient conditions[22] is another strong argument. On the other hand, even if the melting transition is rightly identified, one must reckon the difficulty of the spectrometry method employed for non-contact temperature measurement in laser-heating DAC experiments. Uncertainties due to optical and chromatic aberrations and various other phenomena are then very difficult to estimate.[52] The three hypotheses above might be more or less true altogether and no unique explanation might then be verified.

Finally, there is one last hypothesis that could provide some very surprising explanation of the discrepancies between all the theoretical models (Fig. 9) and the DAC experiments. Both might be true if the melting processes in each case are different. Shock melting and all the theoretical models cited, including ours, correspond to bulk melting. On the other hand, we believe that laser induced melting in DAC is a heterogeneous process because the laser is heating the sample at the boundary with the transparent pressure medium. One might argue that there is now a free surface to permit heterogeneous melting since the sample in DAC experiments is surrounded by a pressure medium (either solid or liquid argon, depending on the pressure and temperature considered); but two recent molecular dynamic studies[53,54] reveal that it is probably not necessary for the boundary to be absolutely free, or to separate solid and liquid of the same nature, to permit heterogeneous melting. In Ref. 50 the authors simply say that the heterogeneity itself is sufficient to ensure the equilibrium melting of the solid if it offers states with higher entropy, no matter the detailed nature of the liquid in contact. As the pressure medium in a DAC, even solid argon, is considerably softer than tantalum $[\theta_D(0) \sim 60$ K and bulk modulus $K \sim 7$ GPa for solid argon whereas $\theta_D(0) \sim 220$ K and $K \sim 200$ GPa for tantalum], atoms of tantalum at the boundary will probably be allowed to reach such higher entropy states. Then we think that the process of melting is most probably "heterogeneous" in the DAC experiment.

Superheating is generally very small at ambient pressure (25 K in the case of silver at ambient pressure), but at higher pressure it can reach many hundreds of Kelvins. However, the highest superheating correction proposed in the past never exceeded 30% of the total bulk melting temperature. Then it is not sufficient in itself to reconcile the theoretical predictions or shock measurements for bulk melting temperatures and the DAC measurement;[22] but we believe that the superheating correction might reach even higher values in the case of tantalum, and probably of the other V A and VI A bcc transition metals which all present similar unusual flat melting curves, an unusually high value of χ at ambient compression, and peculiar anomalies in PDCs at low pressures. A specific study of this question is needed, but some insights are proposed hereafter as open hypothesis. It is well-known that the vibrational properties at the surface of a crystal are influenced by crystallographic orientation of the boundary. For example, the molecular dynamic study by Sorkin[55] on vanadium, another V A bcc transition metal, revealed much larger atomic vibrations on a [1,1,1] surface than on other surfaces or within the bulk. Our study of bulk PDCs tends to show that vanishing at low compressions of the fifth anomaly along the $[0,\xi,\xi]$ direction would tend to increase the thermal vibrations of the crystal if it was not compensated by simultaneous evolution of other anomalies. Then, the discontinuity between pressure medium and tantalum in DAC experiments may strongly affect the equilibrium between these effects and permit larger atomic vibrations along certain boundaries. As a result of such larger atomic vibrations, Sorkin observed on vanadium the development of a thin disordered layer at the surface of the solid, initiating a spreading melting transition of the whole material 300 K lower than the bulk melting temperature, already at ambient pressure. When it is heated, it may then develop, near the surface of the solid bcc tantalum, such a partially disordered surface state of substantially higher energy than the bcc state in the bulk solid. Interestingly enough, such a disordered state was observed at low pressures in Ref. 44 in resolidification simulations of liquid tantalum.

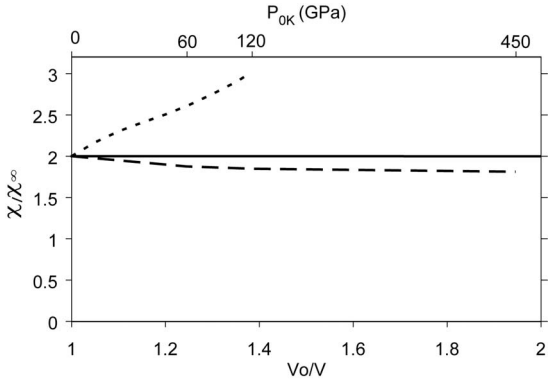

FIG. 10. Evolution of the ratio χ/χ_∞ where χ_∞ represents expected final values in the Thomas-Fermi state according to Burakovsky *et al.* (Refs. 5 and 6). The thick horizontal line is for evolution predicted by Belonoshko *et al.* (Ref. 12). The short dashed line is for values deduced from c_{ij} of this study together with static measurements of T_m (Ref. 22). The long dashed line is for values of $\theta_D(-3,V)/\theta_D(-2,V)$ deduced from the computed PDCs. Pressures at 0 K are reported on the top axis.

IV. CONCLUDING REMARKS

0 K first-principles calculations of c_{ij} and PDCs for bcc Ta presented in this study produced results in global fair agreement with previous experimental and theoretical works. We predict that PDCs are highly influenced by peculiar local changes in the electronic structure between the first few hundred GPa which have hardly any effect on the EOS. This is similar to what was observed on elastic trigonal shear moduli in Gülseren *et al.*[20] Well-known anomalies of ambient PDCs progressively vanish over the first 1000 GPa. Depending on the particular anomaly considered, its vanishing tends either to lower or to increase moment frequencies of atomic vibrations; but as a whole, these variations compensate each other so that, within uncertainties, all $\theta_D(n,V)$ for $n \in [-3,2]$ can be considered proportional above 120 GPa and up to 1000 GPa. This means that the initial Debye model for atomic vibration stands relatively well for this compression range.

As for the ratio $\chi = G_m V/T_m$, as its value is expected to decrease only by a factor of about 2 over 2–4 decades of compression before reaching Thomas-Fermi behavior, it was proposed to take it for a very weak function of density, varying uniformly toward its final value.[12] According to this hypothesis, χ should not be lowered by more than 0.1% over the first 1000 GPa. On the contrary, static measurements of T_m up to 100 GPa by Errandonea[22] make χ increase by more than half in this very limited compression range (Fig. 10).

The first-principles calculations presented here permit one to rule out the hypothesis that this variation is due to a failing of the Debye model for atomic vibration. Indeed $\theta_D(-3,V)/\theta_D(-2,V)$ calculated tends to decrease by a few percent over the first 60 GPa and is constant above within uncertainties up to 1000 GPa (Fig. 10). Then, it is the estimations of T_m themselves that must be addressed.

Uncertainties in the spectrometry method for the noncontact static measurement of temperature can be reevaluated, but it is very unlikely that this can explain all the difference between experimental static T_m and theoretical melting curves. The existence of an extra solid phase that could cause a misinterpretation of melting transition[12] is also excluded in the case of bcc Ta. Then, unless complex anharmonicity was ignored in the various theoretical studies of bcc lattice, experiments in DAC and theoretical *ab initio* calculations of T_m seem both reliable but incompatible. Another hypothesis suggested here is the development of partial disorder near the boundary of the sample in DAC experiments, related to the vanishing of directional phonon anomalies at low pressures.

In the future, it might be interesting to test relations (1) and (2) in transition metals with precise evaluation of anharmonic effects on phonons between 0 K and T_m and with surface phonons modeling. Interesting results are also expectable from molecular dynamic simulations of melting with a coexisting phase method, to avoid superheating, and interatomic potentials specifically constructed to take into account the directional d-electron bounding at different compressions like MGPT potential[44] or modified embedded atom method (MEAM) potential.[56,57]

ACKNOWLEDGMENTS

We want to thank L. Burakovsky and A. Sollier for fruitful discussions and T. Le Bihan and collaborators for the melting experiment at 35 GPa performed with them.

[1] Leonid Burakovsky, Carl W. Greeff, and Dean L. Preston, Phys. Rev. B **67**, 094107 (2003).
[2] M.-H. Nadal and Ph. Le Poac, J. Appl. Phys. **93**, 2472 (2003).
[3] P. Debye, Ann. Phys. **39**, 789 (1912).
[4] F. A. Lindemann, Phys. Z. **11**, 609 (1910).
[5] L. Burakovsky and D. L. Preston, Solid State Commun. **115**, 341 (2000).
[6] L. Burakovsky, D. L. Preston, and R. R. Silbar, Phys. Rev. B **61**, 15011 (2000).
[7] L. Burakovsky, D. L. Preston, and R. R. Silbar, J. Appl. Phys. **88**, 6294 (2000).
[8] L. Burakovsky and D. L. Preston, J. Phys. Chem. Solids **65**, 1581 (2004).
[9] L. Burakovsky, D. L. Preston, and Yi Wang, Solid State Commun. **132**, 151 (2004).
[10] E. Fraizier, M. H. Nadal, and R. Oltra, J. Appl. Phys. **93**, 649 (2003).
[11] E. Fraizier, M. H. Nadal, and R. Oltra, Ultrasonics **40**, 543 (2002).
[12] A. B. Belonoshko, S. I. Simak, A. E. Kochetov, B. Johansson, L. Burakovsky, and D. L. Preston, Phys. Rev. Lett. **92**, 195701 (2004).
[13] N. N. Kalitkin and L. V. Kuzmina, Dokl. Phys. **47**, 778 (2002).
[14] H. Cynn and C.-S. Yoo, Phys. Rev. B **59**, 8526 (1999).
[15] P. Söderlind and J. A. Moriarty, Phys. Rev. B **57**, 10340 (1998).
[16] A. C. Mitchell and W. J. Nellis, J. Appl. Phys. **52**, 3363 (1981).
[17] K. W. Katahara, M. H. Manghnani, and E. S. Fisher, J. Phys. F: Met. Phys. **9**, 773 (1979), and references therein.
[18] A. Dewaele, P. Loubeyre, and M. Mezouar, Phys. Rev. B **69**, 092106 (2004), and references therein.
[19] R. E. Cohen and O. Güseren, Phys. Rev. B **63**, 224101 (2001).
[20] O. Gülseren and R. E. Cohen, Phys. Rev. B **65**, 064103 (2002).
[21] D. Orlikowski, P. Söderlind, and J. A. Moriarty, Phys. Rev. B **74**, 054109 (2006).
[22] D. Errandonea, Physica B **357**, 356 (2005); D. Errandonea, B. Schwager, R. Ditz, C. Gessmann, R. Boehler, and M. Ross, Phys. Rev. B **63**, 132104 (2001); D. Errandonea, M. Somayazulu, D. Haüsermann, and D. Mao, J. Phys.: Condens. Matter **15**, 7635 (2003).
[23] J. M. Brown and J. W. Shaner, in *Shock Waves in Condensed Matter-1983*, edited by J. R. Asay, R. A. Graham, and G. K. Straub (Elsevier, New York, 1984), p. 91.
[24] P. Hohenberg and W. Kohn, Phys. Rev. **136**, B864 (1964).
[25] W. Kohn and L. J. Sham, Phys. Rev. **140**, A1133 (1965).
[26] J. P. Perdew, K. Burke, and M. Ernzerhof, Phys. Rev. Lett. **77**, 3865 (1996).
[27] C. Hartwigsen, S. Goedecker, and J. Hutter, Phys. Rev. B **58**, 3641 (1998).
[28] C. Bercegeay and S. Bernard, Phys. Rev. B **72**, 214101 (2005).
[29] X. Gonze, J.-M. Beuken, R. Caracas, F. Detraux, M. Fuchs, G.-M. Rignanese, L. Sindic, M. Verstraete, G. Zerah, F. Jollet, M. Torrent, A. Roy, M. Mikani, Ph. Ghosez, J.-Y. Raty, and D. C. Allan, Comput. Mater. Sci. **25**, 478 (2002); ABINIT is a common project of the Université Catholique de Louvain, Corning Incorporated, and other contributors (http://www.abinit.org).
[30] R. G. McQueen, S. P. Marsh, J. W. Taylor, J. M. Fritz, and W. J. Carter, in *High Velocity Impact Phenomena*, edited by R. Kinslow (Academic, New York, 1970), p. 293.
[31] W. Holzapfel, Europhys. Lett. **16**, 67 (1991).
[32] T. H. K. Barron and M. L. Klein, Proc. Phys. Soc. London **85**, 523 (1965).
[33] J. A. Moriarty, J. F. Belak, R. E. Rudd, P. Söderlind, F. H. Streitz, and L. H. Yang, J. Phys.: Condens. Matter **14**, 2825 (2002).
[34] X. Gonze, Phys. Rev. B **55**, 10337 (1997).
[35] X. Gonze and C. Lee, Phys. Rev. B **55**, 10355 (1997).
[36] A. D. B. Woods, Phys. Rev. **136**, A781 (1964).
[37] Y. Nakagawa and A. D. B. Woods, Phys. Rev. Lett. **11**, 271 (1963).
[38] G. Grimvall, *Thermophysical Properties of Materials*, enlarged and revised edition (Elsevier, Amsterdam, 1999).
[39] J. E. Lynn, W. J. Trela, and K. Meggers, Nucl. Instrum. Methods Phys. Res. B **192**, 318 (2002).
[40] C. Zener, *Elasticity and Anelasticity of Metals* (University of Chicago Press, Chicago, 1948).

[41] J. C. Slater, Phys. Rev. **57**, 744 (1940).
[42] D. L. Preston and D. C. Wallace, Solid State Commun. **81**, 277 (1992).
[43] Y. Wang, R. Ahuja, and B. Johansson, Phys. Rev. B **65**, 014104 (2001).
[44] J. A. Moriarty, J. F. Belak, R. E. Rudd, P. Söderlind, F. H. Streitz, and L. H. Yang, J. Phys.: Condens. Matter **14**, 2825 (2002).
[45] A. Strachan, T. Cağin, O. Gülseren, S. Mukherjee, R. E. Cohen, and W. A. Goddard III, Modell. Simul. Mater. Sci. Eng. **12**, S445 (2004).
[46] D. C. Wallace, *Statistical Physics of Liquids and Crystals* (World Scientific, Singapore, 2002), p. 236.
[47] R. Boehler, Rev. Geophys. **38**, 221 (2000).
[48] R. Boehler, Hyperfine Interact. **128**, 307 (2000).
[49] M. Ross, R. Boehler, and P. Söderlind, Phys. Rev. Lett. **95**, 257801 (2005).
[50] M. Ross, L. H. Yang, and R. Boehier, Phys. Rev. B **70**, 184112 (2004).
[51] A. B. Belonoshko, R. Ahuja, and B. Johansson, Phys. Rev. B **61**, 11928 (2000).
[52] T. Le Bihan, A. Mesnier, and M. Cadignan (private communication).
[53] A. B. Belonoshko, N. V. Skorodumova, A. Rosengren, and B. Johansson, Phys. Rev. B **73**, 012201 (2006), and references therein.
[54] V. Sorkin, E. Polturak, and J. Adler, Europhys. Lett. **76**, 623 (2006).
[55] S. Sorkin, Ph.D. thesis, Technion University, 2003.
[56] M. I. Baskes, Phys. Rev. B **46**, 2727 (1992).
[57] P. M. Anglade, G. Jomard, G. Robert, and G. Zérah, J. Phys.: Condens. Matter **17**, 2003 (2005).